Benefits and Applications of EHL Analysis in Sealing Technology on the Example of a Hydraulic Step-Seal

Nino Dakov, Christoph Schuele

High-performance seals excel in keeping systems tight in demanding operating conditions, e.g., in high-velocity, high-temperature, and high-pressure applications. To succeed, special care is taken in the design of the contact interface. A key factor for the longevity of the seal is the formation of a stable lubricant film which fully separates the mating surfaces. The generation of load-carrying fluid films in thin lubricated gaps can be described analytically using the theory of elastohydrodynamic lubrication (EHL). In this study, the application of numerical EHL analysis in sealing technology is presented and discussed on the example of a hydraulic step seal. Relevant aspects of modelling the system and evaluating the results are emphasized. Moreover, the benefits of the EHL analysis to assess characteristic performance criteria such as friction and tightness of a sealing system are outlined.

1 Introduction

The generation of load-carrying fluid films in thin lubricated sealing gaps can be approximated using analytical approaches which differ in their accuracy and computational effort. Three main approaches are presented in Figure 1 in a qualitative diagram of their accuracy over the associated computational effort.

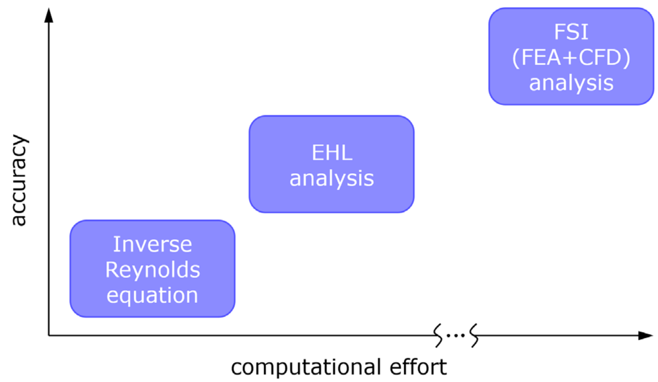

Figure 1: Accuracy vs. computational effort in thin-film lubrication analysis for seals

The inverse theory of hydrodynamic lubrication (IHL), developed by Blok [1] and based on the Reynolds equation for thin lubricated gaps, constitutes the easiest method to estimate the fluid film thickness. The fluid film at outstroke or instroke is assessed via only three input parameters, i.e., the rod speed u at outstroke or instroke, the dynamic viscosity of the fluid η, and the steepest pressure gradient w at outstroke or instroke.

$$h_{\mathrm{rod}} = \sqrt{\frac{2u\eta}{9w}} \tag{1}$$

The IHL stands out due to its simplicity. The associated assumptions, however, limit its applicability in practice. The steepest pressure gradient is calculated from the static contact pressure with assuming that the hydrodynamic pressure is equal to the static contact pressure. The hydrodynamic pressure, however, does not have to be equal to the static one. The only necessary condition is that the hydrodynamic load (or force) is in equilibrium with the static load in order to form a stable fluid film. Another difficulty related to the application of IHL is related to the estimation of the steepest pressure gradient. This is often done by numerical differentiation of a discrete contact pressure profile resulting from a finite element analysis (FEA) simulation. Since the FEA contact stress is only available at the nodes of the mesh, it can be shown that below a certain element edge size the steepest pressure gradient increases linearly with the decrease in the distance between the nodes [2]. In [2] and [3], this limitation is addressed by an extended approach in which the static contact stress from FEA is corrected and smoothed at the inlet region of the contact. Another limiting aspect of IHL is that the theory gives the fluid film thickness at one specific location in the film and does not resolve the complete film thickness along the axial direction. This, in turn, makes it difficult to properly estimate the viscous friction in the contact resulting from the shear stress in the fluid film. Finally, the IHL can only be used for 2D or axissymmetric problems.

The next-efficient method after IHL is the theory of elastohydrodynamic lubrication (EHL). Similar to IHL, EHL analyses utilize the Reynolds equation to model the fluid film in the thin lubricated gap between the seal and the counterface. However, contrary to IHL, an EHL analysis explicitly takes into account the elasticity of the seal. Most commonly, this is achieved via an elastic half space model or an influence coefficient matrix from a FEA [4-5]. While the latter models the material behavior more precisely, e.g., in considering stiffness differences along the contact in the assembled state, the former is much more computationally efficient. The elastic half space is therefore often the method of choice for modelling elastic bodies in EHL. In the EHL analysis, the spatial gap height distribution is resolved together with the hydrodynamic pressure distribution. It should be noted that the hydrodynamic pressure proves to be close but never exactly equal to the static contact pressure. Besides, the EHL results allow an estimation of the friction force as well.

The EHL analysis was among the first analysis types to introduce a so-called fluid-structure interaction (FSI) loop for the iterative calculation of the hydrodynamic pressure and the hydrodynamic film thickness. Nowadays, the term FSI is, however, more frequently used in reference to the coupled FEA / computational fluid dynamics (CFD) analysis. Compared to EHL, a general FSI analysis requires a much higher computational effort. Here, instead of the comparatively simple Reynolds equation, the numerically much more complex Navier-Stokes equations are to be solved hundreds of times in the course of the FSI loop. Similarly, the computationally efficient half space model is swapped for a FEA. A full FSI generally offers the highest possible versatility for the analysis of the fluid flow in the sealing gap. Another upside to using a CFD analysis instead of the Reynolds equation for problems from the field of sealing technology is the possibility to consider a more elaborate mass-conserving cavitation model, e.g., capable of incorporating different types of cavitation such as vaporous and gaseous cavitation. In between EHL and FSI there are different hybrid forms, which couple a half space model and CFD analysis [6] or, alternatively, a FEA and the Reynolds equation [7].

The current work demonstrates some of the benefits and applications of EHL analysis in sealing technology. For reasons of brevity, the focus is on a cross-sectional (2D) example from the field of linear sealing systems. For an overview of simulative studies on linear seals, the reader is referred to [2-3, 8].

2 EHL Theory for 2D Isoviscous Line Contacts

The following section focuses on the essential governing equations for 2D EHL analysis in sealing technology.

Central to the analysis is the Reynolds differential equation for thin lubricating films.

$$\frac{\partial}{\partial x}\left(h^3\frac{\partial p}{\partial x}\right) = 6u\eta\frac{\partial h}{\partial x} \tag{2}$$

Eq. (2) relates the pressure distribution $p(x)$ to the hydrodynamic gap height $h(x)$, the rod speed u, and the viscosity η. Eq. (2) is derived from the Navier-Stokes equations using multiple simplifying assumptions [9]:

- Newtonian lubricant behavior,
- Negligible inertia and volumetric forces, ergo predominant viscous and pressure forces in the fluid film,
- Constant lubricant viscosity and pressure along the height of the film,
- Laminar flow, ergo low Reynolds number,
- Mating surfaces are close to parallel,
- No slip boundary condition at the surfaces.

It can be shown that the above-mentioned assumptions hold quite well for a flow in a narrow gap with the lateral dimensions of the fluid film much larger than its thickness [10]. Thus, for many examples in EHL, the Navier-Stokes equations similar results to the Reynolds equation.

The next important ingredient to the EHL analysis is the half space model for the elastic surface deformation. The total gap height deformation $\Delta h(x)$ follows from the convolution of the single pressure change contributions $\Delta p(x')$ in the entire calculation domain.

$$\Delta h(x) = \frac{1}{\pi E_{\text{red}}}\int_{x'}\Delta p(x')\,\ln(x' - x)^2\,\mathrm{d}x' \quad \text{with} \quad \Delta p = p - p_{\text{FEA}} \tag{3}$$

In Eq. (3), the pressure difference between the static contact pressure p_{FEA} from FEA, which is used as a one-time input to the EHL, and the hydrodynamic pressure p for the current iteration is calculated. Eq. (3) further considers linear elastic deformation with a reduced Young's modulus E_{red}.

$$E_{red} = \left(\frac{1 - v_1^2}{E_1} + \frac{1 - v_2^2}{E_2}\right)^{-1} \tag{4}$$

Eq. (4) incorporates the elasticity parameters – Poisson's ratio v and Young's modulus E – of both surfaces.

It is important to note that the elastic deformation calculated in Eq. (3) cannot be simply neglected since the hydrodynamic pressure is in the same order of magnitude as the stress needed to elastically deform the soft sealing material.

The total gap height results from the static contact geometry from FEA $h_{FEA}(x)$, which is utilized as a second important one-time input from FEA to EHL, as well as the gap height deformation $\Delta h(x)$ from Eq. (3), and a scalar gap height value h_{scalar} separating the two surfaces.

$$h = h_{scalar} + h_{FEA}(x) + \Delta h(x) \tag{5}$$

The last essential equation for the EHL analysis is the so-called load-balance equation. As mentioned in the previous section, for a thin load-carrying film to occur, the dynamic load f needs to balance out the static load f_{FEA}which, in the current case, is another input from FEA.

$$f = \int_x p(x)\,\mathrm{d}x = f_{FEA} = \int_x p_{FEA}(x)\,\mathrm{d}x \tag{6}$$

Specifics to the numerical solution of Eq. (2-6) as well as to the coupling of the fluid flow and elasticity equations are provided in [11]. In the current study, a uniform grid spacing of 4 µm is used for the numerical solution of the hydrodynamic pressure and the hydrodynamic gap height.

It should be noted that, for EHL contacts, the increase in viscosity due to pressure can usually be neglected due to the low reduced Young's modulus of the system. The resulting problem is also referred to as an iso-viscous or soft-EHL contact.

Among the benefits of the presented EHL analysis is the comparatively simple estimation of important performance criteria such as the viscous friction due to shear stress in the fluid film. First, the velocity profile in the lubricated gap is calculated.

$$u(x,z) = \frac{\partial p}{\partial x}\frac{1}{2\eta}\left(z^2 - h(x)\,z\right) + u\left(1 - \frac{z}{h(x)}\right) \tag{7}$$

From Eq. (7), the friction force is estimated.

$$f_R = \int_A \eta \frac{\mathrm{d}u}{\mathrm{d}z}\,\mathrm{d}A \tag{8}$$

It should be noted that Eq. (8) only considers the viscous fluid friction. Therefore, the friction estimation assumes a fully developed fluid film in the sealing contact.

The FEA was carried out in Abaqus. Eq. (2-8) were solved using a self-developed Python program.

3 Analysis of a Hydraulic Step-Seal

The simulation method used in the current work was validated using ellipsometry measurements in a previously published study [4]. The focus was on fluid film thickness at outstroke in a sealing system consisting of a U-cup PU seal and a hard-chrome plated polished rod.

The current study focuses on the analysis of a hydraulic step-seal under a hydraulic pressure. The rod diameter is 50 mm. The sealing material is PTFE grade with mineral fibers. The viscosity of the fluid is 0.1 Pa·s which corresponds to a mineral hydraulic oil of the type HLP 46 at 25 °C. The rod speed is varied between 0.1 and 0.4 m/s. The step-seal is Trelleborg Sealing Solutions' product and has the part number RSK300500. It is energized by a 70 Shore A NBR oring with an inside and cross-section diameters of 56.52 mm and 5.33 mm, respectively. The dimensions of the groove are presented in Figure 2.

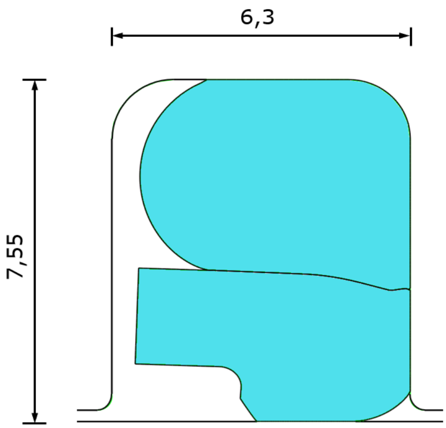

Figure 2: Step-seal RSK300500 with groove dimensions at a rod diameter of 50 mm

In a first step, the step-seal was assembled into the groove in an axissymmetric FEA. In a second step, the FEA results – static contact pressure p_{FEA} and gap height profile h_{FEA} – were used as a one-time input for the EHL analysis of the lubricating film. In the EHL, the surface roughness of the seal and the rod are neglected. For further specifics to the simulation method at use the reader is referred to [4, 11].

In the EHL analysis, fully flooded conditions are assumed on the oil and air side of the seal. This assumption is generally valid for the outstroke case. At instroke, starved lubricating conditions are prevalent in practice. Feuchtmüller et al. [12] show that the film thickness produced by the seal can in certain cases be independent of the amount of fluid at the inlet of the contact. For simplicity, the effect of starved lubrication is neglected in the current study. The simulated film thickness is a theoretical value valid for fully flooded conditions.

The EHL film thickness and hydrodynamic pressure distributions for a rod speed of 0.3 m/s and a hydraulic pressure of 15 and 300 bar are presented in Figure 3 and Figure 4, respectively. A standard linear scaling is used for p and h in the top diagram row. As is visible from both figures, the macroscopic static and dynamic pressure and gap height profiles are quite similar. The only noticeable difference is in the instroke results at 15 bar. To better visualize the differences in the film thickness and the hydrodynamic pressure, a logarithmic scaling is added in the bottom diagram row. The film thickness at the position of the maximum pressure is marked with a black dotted line. Divided by two, this value represents the theoretical film thickness on the rod after one outstroke or instroke [4]. From this value, the theoretical pumping rate can be calculated, refer to [13].

Expectedly, in Figures 3-4, a greater difference between static and hydrodynamic pressure and gap height profiles is visible for the case at instroke. For a retracting rod at instroke, the hydrodynamics in the contact is better which is also evident from the greater film thickness values. Differences between p_{FEA} and p are entirely neglected when the inverse Reynolds equation is used. With IHL, the hydrodynamic pressure is defined as equal to the static one. The higher the viscosity and rod speed – ergo the better the hydrodynamics in the lubricated contact – the greater is the expected difference between IHL and EHL. Nevertheless, even for low speed and viscosity values, the calculation of the steepest pressure gradient in IHL remains highly problematic, leaving EHL as the single universally applicable and computationally efficient option.

Figure 5 shows the theoretical film thickness on the rod after an outstroke or instroke. Note that the theoretical film thickness on the rod is calculated as half the film thickness at the location of the maximal hydrodynamic pressure from Figures 3-4. This relation originates from the conservation of mass in the sealing contact and is valid both for IHL and EHL, see [4].

From Figure 5, it is visible that the film thickness at instroke decreases by a factor of two between 15 and 300 bar. In comparison, the film thickness at outstroke remains almost constant over the hydraulic pressure. The percentage change between each two values of the rod speed is around 20 to 40 % in the investigated rod speed range. A positive difference in single film thickness values from Figure 5, i.e., instroke minus outstroke, corresponds to the theoretical back-pumping capability of the seal. A negative difference between a blue and a red bar is interpreted as leakage expected at a specific instroke to outstroke speed ratio. The results in Figure 5 suggest that, at an instroke and outstroke pressure values of 300 to 15 bar, respectively, the seal is leak-tight up to an instroke to outstroke speed ratio of 1:4.

The calculated friction force normalized by the rod circumference is presented in Figure 6. The results show a strong dependence of the friction on the hydrodynamic gap height and the hydraulic pressure. Both a decrease in the gap height, e.g., at outstroke compared to instroke, and an increase in the hydraulic pressure lead to an

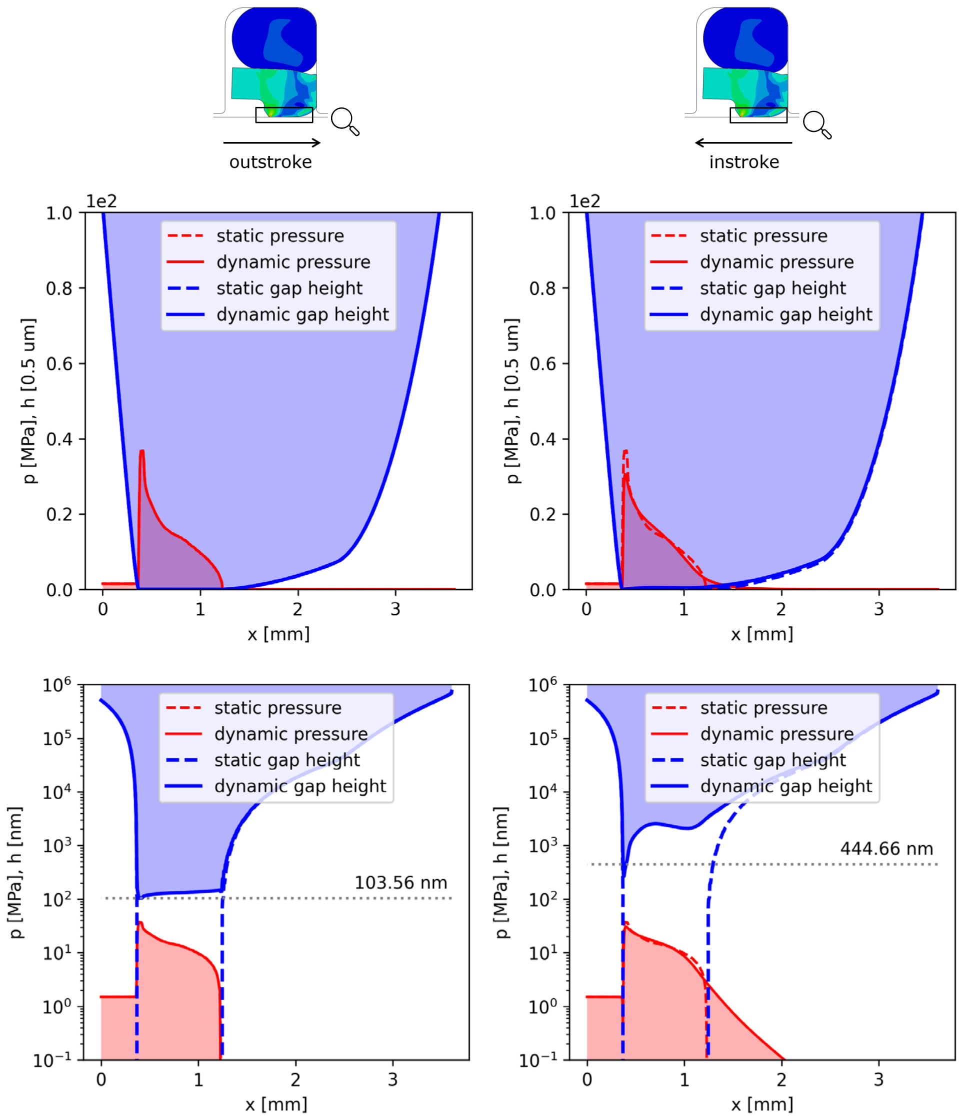

Figure 3: EHL film thickness and hydrodynamic pressure distribution for a hydraulic pressure of 15 bar and rod speed of 0.3 m/s, linear scaling (top) and logarithmic scaling (bottom)

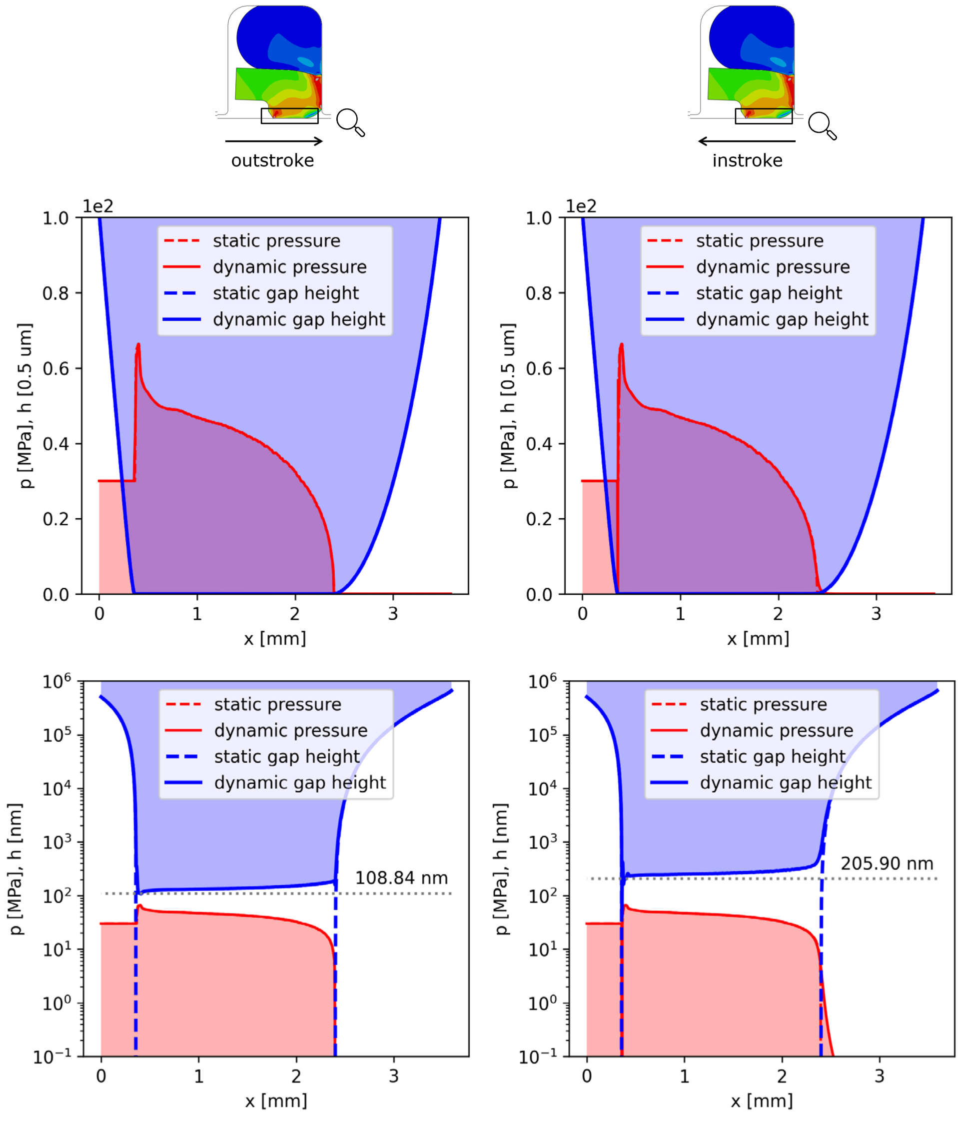

Figure 4: EHL film thickness and hydrodynamic pressure distribution for a hydraulic pressure of 300 bar and rod speed of 0.3 m/s, linear scaling (top) and logarithmic scaling (bottom)

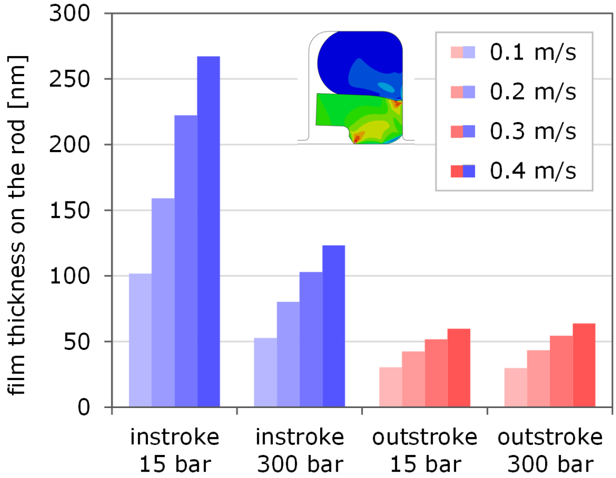

Figure 5: EHL film thickness of step-seal at outstroke and instroke over the hydraulic pressure and rod speed

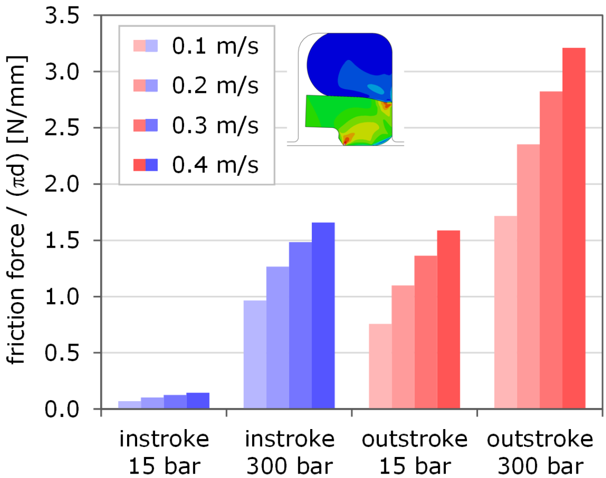

Figure 6: EHL friction force of step-seal at outstroke and instroke over the hydraulic pressure and rod speed

increase in the friction force. Here, the increase in hydraulic pressure affects the friction by enlarging the width of the thin lubricated sealing gap and thus increasing the fluid area with a high shear stress. A comparison with already published values is used to validate the order of magnitude of the simulated friction force values. In

[14], a total normalized force between 3 and 3.3 N/mm was measured on two step-seals of the same type in face-to-face arrangement. In the experiment, the conditions were similar to the current study with a hydraulic pressure of 300 bar, as well as rod speed and viscosity of 0.2 m/s and ca. 0.05 Pa·s, respectively. At a rod speed of 0.1 m/s and a viscosity of 0.1 Pa·s ($u \cdot \eta$ = 0.01 Pa·m and thus similar lubricating conditions to the experiment), the EHL analysis gives a total normalized friction force of 2.7 N/mm. However, it should be noted that the quantitative estimation of the friction force requires considering that, at instroke, the amount of fluid is limited to the film thickness which was produced at outstroke. Therefore, for a retracting rod in practice, a higher friction force is to be expected than the simulated values. Furthermore, in the current study, the effect of surface roughness is not considered. Expectedly, to obtain quantitative results on the film thickness and the friction in the contact, the surface finish of both the seal and the rod is to be taken into account as well.

The greatest potential of a EHL is seen in the fast and efficient comparative analysis of different designs. Elucidating the overall impact of the design on the performance of the seal is an achievable goal for which qualitative EHL results are well obtainable. To carry out a quantitative EHL analysis, an in-depth model of the seal including surface roughness effects and mixed lubrication model is required.

4 Summary and Conclusion

The focus of the current study was on highlighting the benefits of EHL analysis for improving the understanding of the sealing performance. A hydraulic step seal served as an example for the film thickness and friction analysis. The EHL analysis proved to be a computationally efficient, stable, and versatile method to acquire plausible results for the film thickness and the friction force in the sealing contact depending on the hydraulic pressure and the rod speed. The EHL analysis can thus be utilized for the qualitative comparison and the numerical optimization of different sealing designs for demanding applications.

5 Nomenclature

A	Contact area	[m^2]
$E_{1,2}$	Young's modulus of rod and seal	[Pa]
E_{red}	Reduced Young's modulus	[Pa]
f	Hydrodynamic load	[N]
f_{FEA}	Static contact load from FEA	[N]
f_{R}	Friction force	[N]
h	Hydrodynamic film thickness	[m]
h_{FEA}	Static gap height profile from FEA	[m]
h_{rod}	Film thickness on the rod after an instroke or outstroke	[m]
h_{scalar}	Scalar film thickness from film thickness Eq. (5)	[m]

Δh	Gap height deformation	[m]
p	Hydrodynamic pressure	[Pa]
p_{FEA}	Static contact pressure	[Pa]
u	Rod speed	[m/s]
w	Steepest pressure gradient	[Pa/m]
x	Axial coordinate	[m]
z	Radial (height) coordinate	[m]
η	Dynamic viscosity	[Pa·s]
$v_{1,2}$	Poisson's ratio of rod and seal	[-]

6 References

[1] Blok, H. *Inverse Problems in Hydrodynamic Lubrication and Design Directives for Lubricated Flexible surfaces*. In Proceedings of the International Symposium on Lubrication and Wear, Houston, TX, USA, 1963.

[2] Kaiser, F. *Ein Simulationsmodell zur Analyse des Schmierfilms von Stangendichtungen*. Dissertation, 2015, Institute of Machine Elements, Gears and Tribology, Technical University Kaiserslautern.

[3] Crudu, M.; Fatu, A.; Cananau, S.; Hajjam, M.; Pascu, A.; Cristescu, C. *A numerical and experimental friction analysis of reciprocating hydraulic "U" rod seals*. Proc. Inst. Mech. Eng. Part J J. Eng. Tribol. 2012, 226, 785–794. https://doi.org/10.1177/1350650112445973

[4] Feuchtmüller, O.; Dakov, N.; Hörl, L.; Bauer, F. *Remarks on Modeling the Oil Film Generation of Rod Seals*. In: Lubricants, 2021, 9, 95. https://doi.org/10.3390/lubricants9090095

[5] Salant, R. F.; Yang, B.; Thatte, A. *Simulation of Hydraulic Seals*. In: Proceedings of the Institution of Mechanical Engineers, Part J: Journal of Engineering Tribology, 2010, https://doi.org/10.1243/13506501JET709

[6] Tošić, M.; Larsson, R.; Jovanović, J.; Lohner, T.; Björling, M.; Stahl, K. *A Computational Fluid Dynamics Study on Shearing Mechanisms in Thermal Elastohydrodynamic Line Contacts*. Lubricants 2019, 7, 69. https://doi.org/10.3390/lubricants7080069

[7] Angerhausen, J. *Physikalisch motivierte, transiente Modellierung translatorischer Hydraulikdichtungen*. Dissertation, 2020, Institute for Fluid Power Drives and Systems, RWTH Aachen, Germany. https://doi.org/10.18154/RWTH-2020-09585

[8] Nikas, G. K. *Profile Optimization of Hydraulic, Polymeric, Sliding Seals by Minimizing an Objective Function of Leakage, Friction and Abrasive Wear*. Lubricants 2020, 8, 40. https://doi.org/10.3390/lubricants8040040

[9] Gohar, R.: *Elastohydrodynamics*. World Scientific, 2001.

[10] Dobrica, M.; Fillon, M. B. *About the Validity of Reynolds Equation and Inertia Effects in Textured Sliders of Infinite Width.* Proceedings of the Institution of Mechanical Engineers, Part J: Journal of Engineering Tribology 223 (1), 2009. https://doi.org/10.1243/13506501JET433

[11] Dakov, N. *Elastohydrodynamische Simulation von Wellendichtungen am Beispiel der PTFE-Manschettendichtung mit Rückförderstrukturen*. Dissertation, 2020, Institute for Machine Components, University of Stuttgart, Germany. http://dx.doi.org/10.18419/opus-10997

[12] Feuchtmüller, O.; Hörl, L.; Bauer, F. *An Empirical Study on the Friction of Reciprocating Rod Seals at Predefined Lubrication Conditions and Shear Rates*. In: Lubricants, 2022, 10, 56, https://doi.org/10.3390/lubricants10040056

[13] Müller, H. K.; Nau, B. S. *Fluid Sealing Technology: Principles and Applications*. M. Dekker, 1998.

[14] Roepstorff, S., Larsen, T., Jordan, H. *New PTFE-based Material for Hydraulic Seal Applications*, In: 16th International Sealing Conference Stuttgart 2010, Stuttgart, Germany, pp. 238-247, October 12-13, 2010.

7 Authors

Trelleborg Sealing Solutions Germany GmbH

Schockenriedstr. 1, 70565 Stuttgart, Germany:

Dr.-Ing. Nino Dakov

ORCID 0000-0002-0989-9943, nino.dakov@trelleborg.com

M.Sc. Christoph Schuele

ORCID 0000-0002-2762-4409, christoph.schuele@trelleborg.com